

## **CHAPTER 3**

### **SP-Driven Reduction Catalytic Reactions**

#### **3.1 SP-Driven Reduction Catalytic Reactions in Atmosphere Environment**

##### **3.1.1 SP-Driven Reduction Catalytic Reactions by SERS in Atmosphere Environment**

In the above, the author described the dimerization oxidation reactions about the PATP to DMAB from the perspective of chemical thinking, and in this part, the conversion about the PNTP to DMAB will be mainly introduced, which was a reduction reaction. And this indicated that SPs might play different roles in inducing chemical reactions, which might broaden the research field of plasmon driven catalytic reactions to a large extent. This section will introduce another model of the plasmon driven reactions, which was to reduce PNTP to DMAB. In addition, it was generally believed that the hot electrons generated by plasmon decay, that is, holes, could drive this kind of chemical reactions.

As was demonstrated in the Fig. 14(a), three major strong Raman signals appeared at  $1099\text{ cm}^{-1}$ ,  $1331\text{ cm}^{-1}$  and  $1574\text{ cm}^{-1}$  in the NRS spectrum of the measured 4NBT powder, and Fig. 14(b) displayed the simulated NRS spectrum about the 4NBT. Furthermore, the theoretical results revealed that there were two nearly degenerate Raman signals near the wavenumber of  $1100\text{ cm}^{-1}$ . The

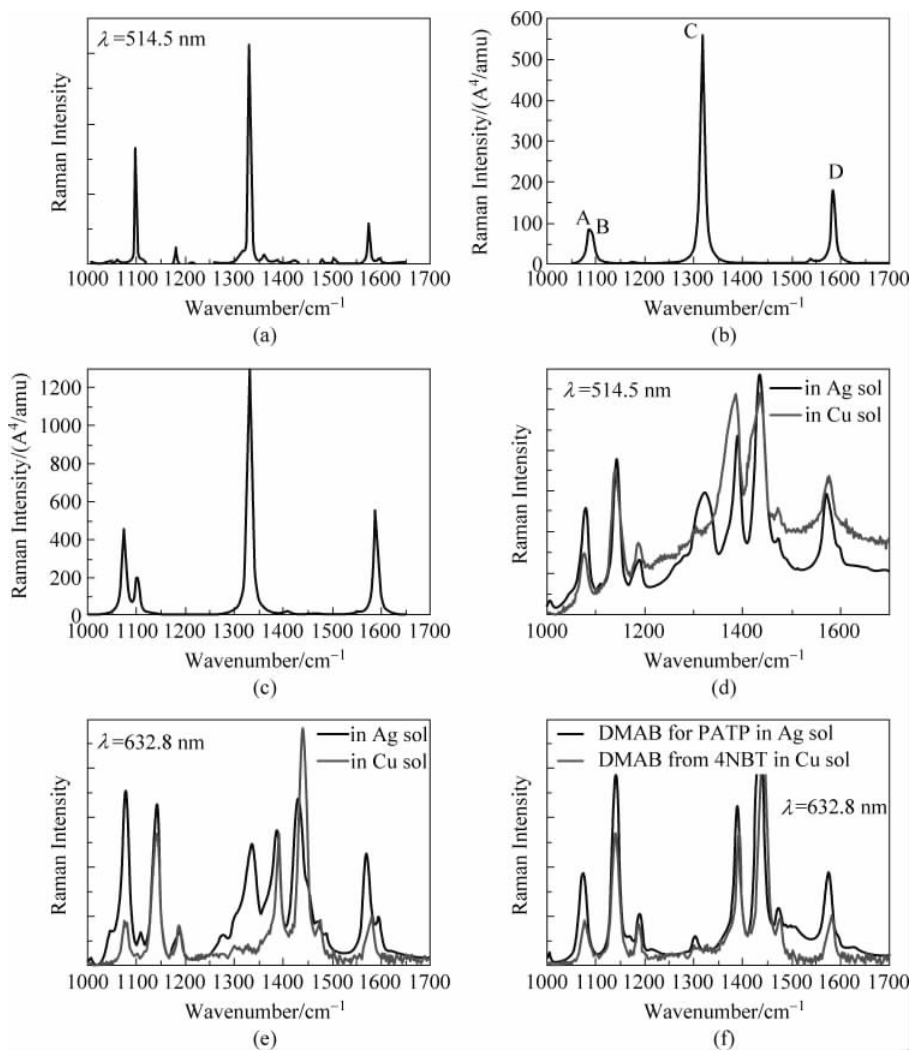


Fig. 14 (a) The NRS spectrum of 4NBT powder; (b) The simulated NRS spectrum of 4NBT; (c) The simulated SERS of 4NBT adsorbed on Ag<sub>5</sub> cluster; (d), (e) The experimental SERS spectrum of DMAB produced from 4NBT excited at 514.5 nm and 632.8 nm in Ag and Cu sols, respectively; (f) The experimental SERS of DMAB produced from PATP<sup>[2,3]</sup>, and from 4NBT by surface photochemistry reactions<sup>[32]</sup>

(For colored figure please scan the QR code on page 2)

author could see the visualization of the four vibration modes about the NRS spectrum in the Fig. 14(b). According to research, the Raman peak A was a S—C stretching vibration shown in Fig. 14(b). The Raman peak C was  $\nu_s(\text{NO}_2)$  stretching vibration of the benzenyl ring, and the Raman peak D was the C=C stretching vibration about it. Figure 14(c) displayed the simulated SERS spectrum of 4NBT adsorbed on silver clusters, and this was done before measuring the SERS of 4NBT. It could be seen from the figure that there were three stronger Raman signals, and the distribution of the SERS spectrum about the 4NBT was very similar to the distribution of the NRS spectrum in the 4NBT powder in Fig. 14(a). At last, the Fig. 14(d) displayed the SERS spectrum about the 4NBT in an Ag and Cu sol measured at an incident wavelength was 514.5 nm, and the Fig. 14(e) displayed an incident laser with 632.8 nm. The authors were able to find that the curves of the SERS spectra were significantly different from a simulated SERS spectrum about the 4NBT. As displayed in Figs. 14(d) and (e), in the Ag or Cu sol, there were three strong Raman peaks at the wavenumbers of  $1142\text{ cm}^{-1}$ ,  $1387\text{ cm}^{-1}$ , and  $1432\text{ cm}^{-1}$ , respectively, and there were several strengths slightly larger around those Raman peaks. It was worth noting that the Raman peak at wavenumber of  $1331\text{ cm}^{-1}$  disappeared in the Cu sol, however the Raman peak in the Ag sol still exists. This indicated that a complete reactions occurred in the Cu sol and a partial reactions occurred in the Ag sol, which proved that the Cu sol was a relatively good reactions environment for this kind of the surface photochemical reactions.

In order to better reveal the properties of the experimental SERS spectra, the authors compared the spectra in Figs. 14(d) and (e) with the SERS spectra about the DMAB generated from PATP through surface photochemical reactions<sup>[2,3]</sup>. Based on Fig. 14(f), the authors observed that the experimental SERS spectra about DMAB generated from the PATP through surface photochemical reactions were very similar to those in Figs. 14(d) and (e), particularly in the Cu sol, the spectra of the two were almost the same<sup>[2]</sup>.

Therefore, the authors could conclude that DMAB molecules were produced in two ways, from PATP production and 4NBT production. In Fig. 14(d) to Fig. 14(f), under the condition that wavenumber was  $1432\text{ cm}^{-1}$ , it was the  $\text{N}=\text{N}$  stretching vibration about the DMAB<sup>[2]</sup>, which indicated the generation about DMAB molecules.

To further explore the factors affecting the surface catalytic reduction about 4NBT to DMAB, the authors attempted to control the reactions with different laser wavelengths, substrates, and time scales. To begin with, Au, Ag and Cu films were produced by using a vacuum electron beam evaporator. In addition, surface catalytic reduction about the 4NBT was measured using SERS spectroscopy under different experimental environments. Third, the authors could conclude that the optimal experimental conditions needed to be reasonably selected to accelerate or inhibit the rate of reactions.

A substrate for SERS detected was produced by evaporating Au, Ag, and Cu metal onto Si by using a vacuum electron beam evaporator under HV. The authors needed to carefully control the evaporation conditions so that the average thickness of the different metal layers produced was 50 nm. Figures 15 (a)—(c) displayed the atomic force microscopy (AFM) image of the substrate surface of different metals. The lighter the color of the image, the coarser the

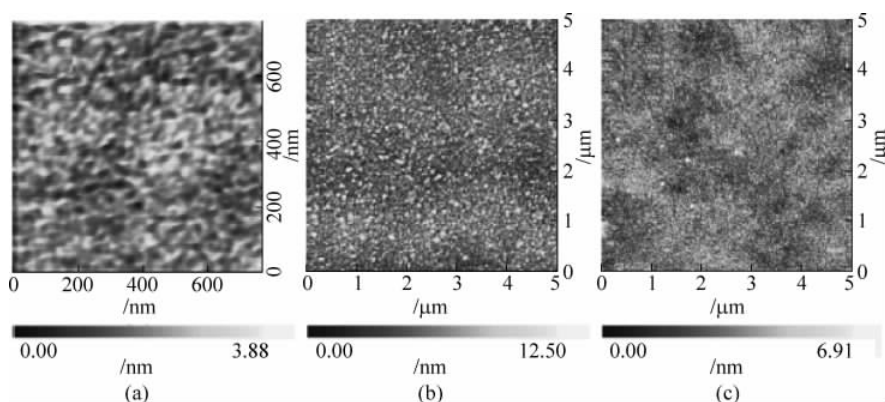


Fig. 15 AFM picture of the (a) Au, (b) Ag, and (c) Cu films<sup>[43]</sup>

(For colored figure please scan the QR code on page 2)

metal surface, so the surface of the metallic Cu could be found to be the roughest. Here, the authors measured the Au, Ag and Cu films, the average roughness values were 0.56 nm, 2.03nm and 1.04 nm, respectively. Further, the surface morphology of the Au, Ag and Cu films was characterized through scanning electron microscopy (SEM) images. These SEM images of Au, Ag, and Cu films were shown in Figs. 16 (a)—(c), respectively. Figure 16 (d) displayed an SEM image of NPs having an average diameter of about 110 nm.

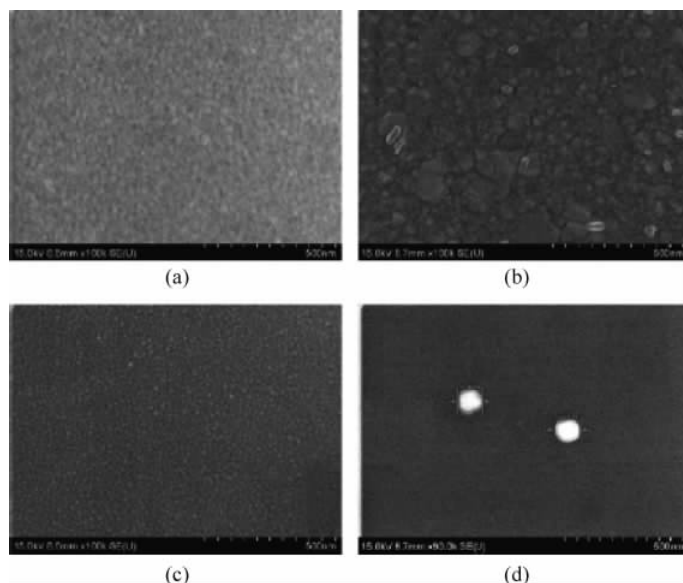


Fig. 16 SEM images of the (a) Au, (b) Ag, and (c) Cu films and (d) Ag NPs<sup>[43]</sup>

To begin with, the Au, Ag and Cu films were immersed in a 4NBT solution of  $1 \times 10^{-5}$  mol/L in ethanol for a period of more than 5 hours. In addition, the metal film was then passed through acetone, ethanol and deionized water in sequence and washed separately for 3 minutes, respectively. Last but not least, these metal films were dried with nitrogen, and Ag NPs were dropped on the metal films to produce hot spots between the films and the NPs. The above method of preparing a NPs-molecular-film junction could enhance the Raman intensity significantly<sup>[44]</sup>. Here, the authors measured the Raman spectra about the 4NBT on Au, Ag and Cu films by using a Renishaw in Via

Raman system equipped with an integral microscope. The device used lasers with wavelengths of 632.8 nm and 514.5 nm.

In previous experimental studies, the direct experimental evidence for the formation of DMAB by surface catalytic dimerization about the 4NBT was that the Raman signal at  $1331\text{ cm}^{-1}$  in the Cu sol disappeared completely. And Raman peaks appeared near  $1387\text{ cm}^{-1}$  and  $1432\text{ cm}^{-1}$ , corresponding to the vibration modes of  $a_{g_{16}}$  and  $a_{g_{17}}$ , respectively. This was associated with  $\text{—N=N—}$  of the DMAB<sup>[32]</sup>. As was demonstrated in the Fig. 17(a), under the irradiation of incident light with 632.8 nm, the SERS profiles and intensity about the molecules adsorbed on the Cu film hardly changed with the reactions time exceeding two hours, which was mainly due to the  $\nu_s(\text{NO}_2)$  of the 4NBT. Therefore, in the above case, surface catalytic reduction by 4NBT did not occur to the DMAB molecule. In contrast, the Fig. 17(b) displayed that when the wavelength of incident light became 514.5 nm, the SERS profiles and intensity about molecules adsorbed on the Cu film changed significantly, and the  $\nu_s(\text{NO}_2)$  Raman intensity of 4NBT disappeared within 2 minutes, and the Raman intensity of the  $a_{g_{16}}$  and  $a_{g_{17}}$  vibration modes related to  $\text{—N=N—}$  of DMAB occurred at a time of 1 minute. Therefore, under the excitation of incident light with 514.5 nm, 4NBT was rapidly reduced to DMAB on the Cu film. The above experiments revealed that for a wavelength-dependent surface-catalyzed reactions, for example, the barrier  $V_{pb}$  of the above reactions should be greater than 1.599 eV on the Cu film, since the energy of the incident light with a wavelength of 632.8 nm was 1.959 eV, so the excitation of the incident light having a wavelength of 632.8 nm did not react.

As was demonstrated in the Fig. 17(c), under the excitation of incident light with a wavelength of 632.8 nm, the DMAB on the Au film could not be formed by 4NBT for up to 2.5 hours because the Raman intensity about the  $\nu_s(\text{NO}_2)$  of 4NBT did not change. And in Fig. 18, the distribution of the local electric field about the Ag NPs-Au film with incident laser of 632.8nm. Therefore, the Fig. 17(d) displayed that there was almost no Raman peak

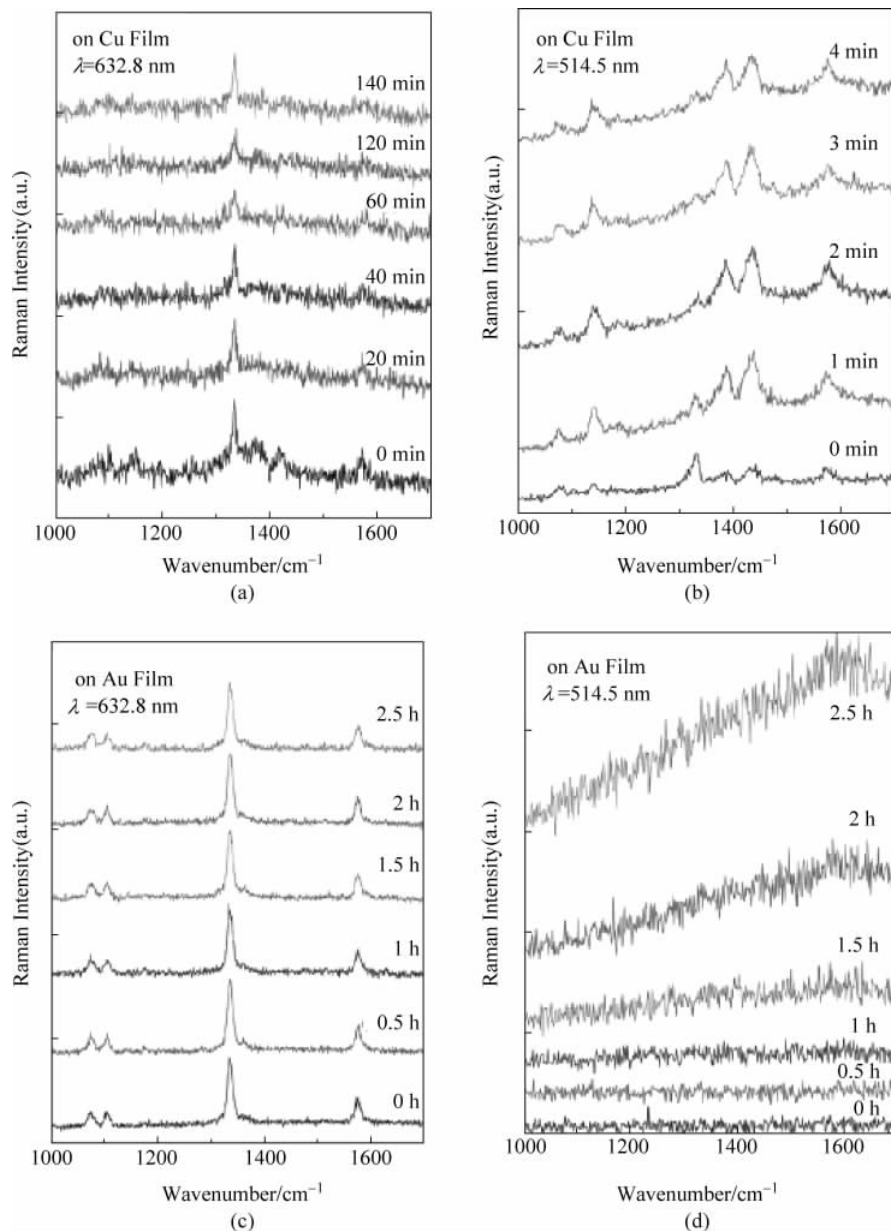


Fig. 17 SERS spectra of 4NBT at the junction of Ag NPs on the Cu, Au, and Ag films system

(a), (b) On the Cu film at incident wavelengths of 632.8 nm and 514.5 nm, respectively;  
 (c), (d) On the Au film at incident wavelengths of 632.8 nm and 514.5 nm, respectively;  
 (e), (f) on the Ag film at incident wavelengths of 632.8 nm and 514.5 nm, respectively<sup>[43]</sup>

(For colored figure please scan the QR code on page 2)

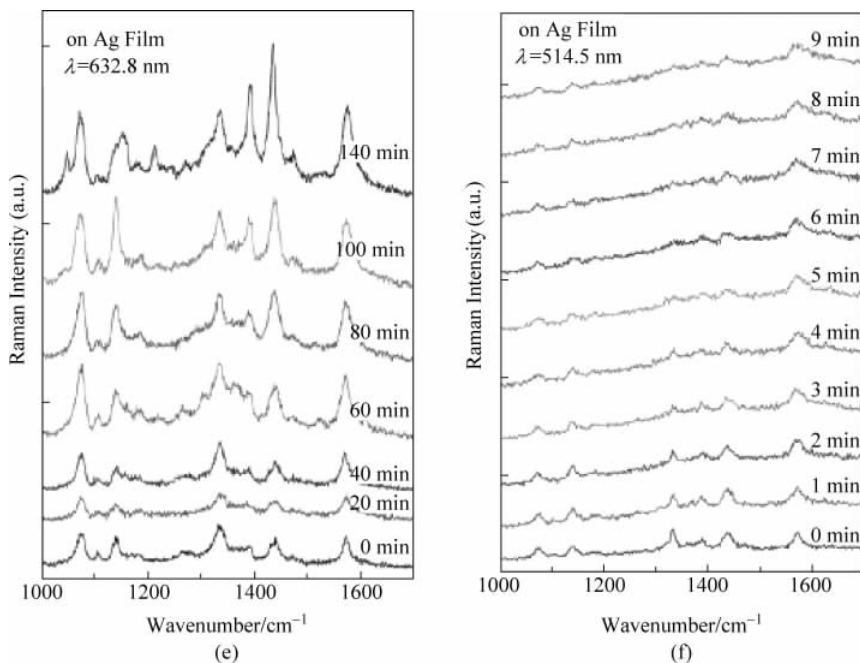


Fig. 17 (Continued)

after 2.5 hours, which indicated that the Au film was not the optimum substrate under the irradiation of incident light having a wavelength of 514.5 nm, because the use of this incident light caused the coupling between the conduction electrons and the electronic transition between the bands to significantly reduce the quality about the plasmon resonance of the Au metal surface<sup>[43]</sup>.

The authors further researched factors affecting the surface catalytic reactions about molecules adsorbed on the Ag film, such as laser wavelength and reactions time. As was demonstrated in the Fig. 17 (e), the Raman intensity of the vibration modes of  $a_{g_{16}}$  and  $a_{g_{17}}$  was much weaker compared to the  $\nu_s(\text{NO}_2)$  Raman intensity about the 4NBT in 60 minutes under incident light with 632.8 nm. With the laser irradiation time rose, the Raman intensity of vibration modes about the  $a_{g_{16}}$  and  $a_{g_{17}}$  gradually increased. When the reactions time exceeded 80 minutes, the Raman intensity about the vibration



modes of  $a_{g16}$  and  $a_{g17}$  became stronger as compared with the Raman intensity of  $\nu_s(\text{NO}_2)$  about the 4NBT. When the reactions was carried out for 140 minutes, the Raman intensity about the vibration modes of  $a_{g16}$  and  $a_{g17}$  was significantly enhanced compared to the Raman intensity of  $\nu_s(\text{NO}_2)$  about the 4NBT. As displayed in the Fig. 17(f), compared with the reactions time under the irradiation conditions of incident light with 632.8 nm, the reactions time under the irradiation of incident light with 514.5 nm was very short, it could be done in just 5 minutes.

Note that under the irradiation of incident light with 632.8 nm, the authors could not observe the surface catalytic reduction about 4NBT to DMAB on Au and Cu films in time-dependent SERS spectra. Nevertheless, as displayed in the Fig. 18, this surface-catalyzed reaction occurred in Au sol and Cu sol under the same incident light irradiation conditions<sup>[45]</sup>. The authors analyzed the above results because the specific surface area of Au NPs and Cu microparticles was very large compared to Au and Cu films, and the hot sites in the NPs were more than a single hot site in NPs-molecular-Au film junction. Therefore, the value of  $|M|^2$  about the

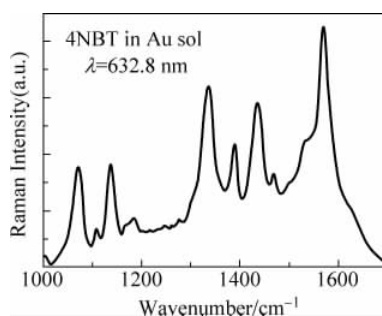


Fig. 18 SERS spectrum of 4NBT in an Au sol at an incident wavelength of 632.8 nm<sup>[43]</sup>

EM enhanced in the nanogap of the NPs-molecular-Au film junction was  $5.1 \times 10^5$ . The Fig. 19 displayed the local electric field intensity distribution of a Ag NPs-Au film irradiated with incident light with 632.8 nm. Note that since the  $k$  about the electric field and the primary collecting the Raman signal were perpendicular to the surface, the effective EM enhancement of collecting the SERS signal was weak. Previous studies had shown that in TERS, the optimal angle between  $k$  and the surface from which the Raman signal was collected was  $60^\circ$ . Therefore, the authors could conclude that the reactions rate was related to the laser wavelength, laser power, reactions atmosphere and so on.

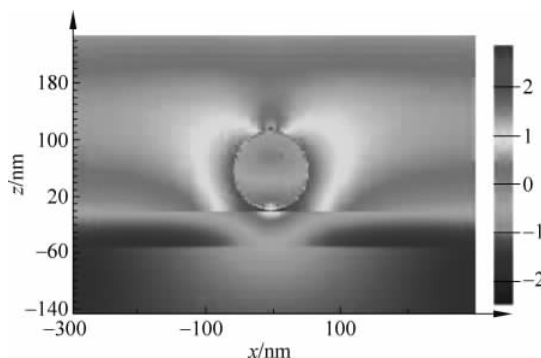


Fig. 19 The Ag NPs-Au film at an incident wavelength of 632.8 nm<sup>[43]</sup>  
(For colored figure please scan the QR code on page 2)

Studies had demonstrated that the reduction about the DMAB to PATP in the environment with only water vapor was induced through hot-electrons produced by SP decay. Through this work, it could be concluded that SPs played different roles in chemical reactions; in oxidation reactions plasmonic heating and sources of hot electrons in reduction reactions. Previous studies had shown that by controlling the pH of the reactions medium and nitrite, the reactions rate and reactivity could be controlled.

The authors could understand that the intensity of SPs generated on the surface about the metal nanostructure was dependent on the wavelength and power of the incident laser strongly, such as Au and Ag, the matching laser wavelength and higher laser power with the SP resonance of the metal usually generated a stronger SP. The mechanism about this reduction reaction was explained in previous studies<sup>[46]</sup>. Note that it was not possible to find this reduction in an oxygen atmosphere where the laser power was weak, however it was possible to give a sufficiently high laser power first, which indicated that oxygen might quench limited thermal electrons at low laser power. Therefore, this prohibited the transition from PNTP to DMAB<sup>[47]</sup>. Here the authors compared the SERS spectra of a set of materials by density functional theory (DFT), such as PNTP, PATP, DMAB and benzenethiol. The results showed that the conversion of PNTP to PATP in water or hydrogen